

# EPR characterization of half-integer-spin iron molecule-based magnets

Saiti Datta<sup>a</sup>, Amalia Betancur-Rodriguez<sup>a</sup>, Sheng-Chiang Lee<sup>a</sup>, Stephen Hill<sup>a,\*</sup>,  
Dolos Foguet-Albiol<sup>b</sup>, Rashmi Bagai<sup>b</sup>, George Christou<sup>b</sup>

<sup>a</sup> Department of Physics, University of Florida, Gainesville, FL 32611-8440, USA

<sup>b</sup> Department of Chemistry, University of Florida, Gainesville, FL 32611-7200, USA

Received 7 November 2006; accepted 9 November 2006

Available online 17 November 2006

## Abstract

We report single crystal high-frequency electron paramagnetic resonance studies of two recently discovered half-integer Fe<sub>7</sub> complexes: [Fe<sub>7</sub>O<sub>3</sub>(O<sub>2</sub>CBu<sup>t</sup>)<sub>9</sub>(mda)<sub>3</sub>(H<sub>2</sub>O)<sub>3</sub>] (**1**) and [Fe<sub>7</sub>O<sub>4</sub>(O<sub>2</sub>CPh)<sub>11</sub>(dmem)<sub>2</sub>] (**2**). The obtained spectra confirm spin  $S = 5/2$  ground states for both complexes. On the basis of detailed frequency and field orientation dependent studies, we find that complex **1** is a single-molecule magnet (uniaxial zero-field-splitting parameter,  $D < 0$ ) while complex **2** is not ( $D > 0$ ). The EPR linewidth for complex **1** is considerably narrower in comparison to spectra obtained for other single-molecule magnets, suggesting the possibility of reduced decoherence from nuclear spins (<sup>56</sup>Fe has no nuclear moment).

© 2006 Elsevier Ltd. All rights reserved.

**Keywords:** Single-molecule magnets; Nanomagnet; Electron paramagnetic resonance; Quantum tunneling; Iron

## 1. Introduction

Half-integer-spin iron single-molecule magnets (SMMs) are of great interests because they exhibit greatly suppressed quantum tunneling of magnetization (QTM) [1,2] at zero magnetic field, and because naturally abundant <sup>56</sup>Fe has no nuclear spin ( $I = 0$ ) which could act as a major source of decoherence [3]. Consequently, although many half-integer-spin manganese (with  $I = 5/2$ ) SMMs [4,5] have been studied, half-integer iron SMMs may be expected to provide important advantages for studies of coherent quantum magnetization dynamics with potential applications in quantum information processing (quantum computing).

Here, we report high-frequency electron paramagnetic resonance (HF-EPR) studies of two half-integer Fe<sub>7</sub> complexes [Fe<sub>7</sub>O<sub>3</sub>(O<sub>2</sub>CBu<sup>t</sup>)<sub>9</sub>(mda)<sub>3</sub>(H<sub>2</sub>O)<sub>3</sub>] (**1**) and [Fe<sub>7</sub>O<sub>4</sub>(O<sub>2</sub>CPh)<sub>11</sub>(dmem)<sub>2</sub>] (**2**). The main purpose of this work is

to precisely determine the zero-field-splitting (zfs) parameters of the molecules based on a giant spin approximation.

## 2. Experimental

The complexes were synthesized from the reaction of basic iron carboxylates with alcohol based ligands. Orange crystals of complex **1** were obtained from the reaction of [Fe<sub>3</sub>O(O<sub>2</sub>CBu<sup>t</sup>)<sub>6</sub>(H<sub>2</sub>O)<sub>3</sub>](NO<sub>3</sub>) with mdaH<sub>2</sub> in a 1:3 molar ratio in MeCN with a 43% yield. Orange crystals of complex **2** were obtained from the reaction of [Fe<sub>3</sub>O(O<sub>2</sub>CPh)<sub>6</sub>(H<sub>2</sub>O)<sub>3</sub>](NO<sub>3</sub>) with dmeh in a 1:2 molar ratio in MeCN with a 45% yield. Full details will be provided elsewhere [6,7]. Both complexes are thought to have spin ground states of  $S = 5/2$ . The structures of the complexes **1** and **2** are shown in Figs. 1(a) and (b), respectively. The structural details can be found elsewhere [6,7].

HF-EPR measurements were performed on single crystals (one at a time) at various frequencies from 50 to 200 GHz, with the DC magnetic field applied along different crystallographic directions. The crystals were removed from the mother liquor and immediately protected with

\* Corresponding author. Tel.: +1 352 392 5711.

E-mail address: [hill@phys.ufl.edu](mailto:hill@phys.ufl.edu) (S. Hill).

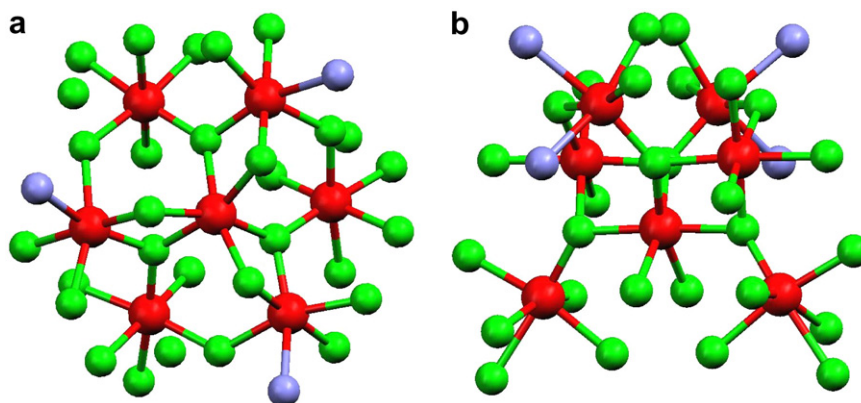


Fig. 1. (a) Structure of complex **1**; hydrogen atoms and t-butyl groups have been omitted for clarity. The  $C_3$  symmetry axis is out of the page. Color code:  $\text{Fe}^{\text{III}}$  – red; O – green; N – blue. (b) Structure of complex **2**; hydrogen atoms and phenyl rings have been omitted for clarity. Color code:  $\text{Fe}^{\text{III}}$  – red; O – green; N – blue. (For interpretation of the references in color in this figure legend, the reader is referred to the web version of this article.)

grease to prevent solvent loss during cooling in helium gas at atmospheric pressure. A sensitive cavity-perturbation technique and a millimeter-wave vector network analyzer (MVNA) were used to detect the EPR signals (details are given elsewhere [8,9]). The spectra were obtained at fixed microwave frequencies and temperatures while sweeping the DC magnetic field.

### 3. Data and discussion

The magnetic axial direction of complex **2** was hard to determine due to its low symmetry. Therefore, single-axis angle-dependent HF-EPR studies only allow us to locate the plane perpendicular to the axial direction. Extensive measurements at various temperatures and frequencies were then performed with DC fields applied in this plane to determine the ground state transitions and zero-field splitting (zfs) parameters in the spin Hamiltonian,  $\hat{H} = D\hat{S}_z^2 + E(\hat{S}_x^2 - \hat{S}_y^2) + g\mu_B\vec{B} \cdot \hat{S}$ .

Fig. 2 shows temperature-dependent spectra for complex **2** taken at 197 GHz, with the field in the ( $xy$ -) plane perpendicular to the axial ( $z$ -) direction. A total of five main peaks are observed, thus confirming the  $S = 5/2$  ground state of the molecule. Each peak exhibits fine structures which are most probably caused by weak disorder, which leads to distributions in the zfs parameters. The lowest field peak (labeled a) corresponds to the excitation from the ground state within the  $S = 5/2$  multiplet, since it clearly becomes stronger upon lowering the temperature. Based upon this observation, we conclude that the magnetic anisotropy of complex **2** is of the easy-plane type, i.e. it possesses a positive  $D$  value. The inset to Fig. 2 displays the Zeeman diagram for a spin  $S = 5/2$  system with a positive  $D$  value and the field applied within the easy plane. The five observed transitions (a–e) are indicated in the inset.

We note that it is possible to fit the spectra in Fig. 2 assuming a negative  $D$  value. However, we cannot account for the angle dependence on the basis of such an assign-

ment. Consequently, it is clear that  $D$  must be positive. Further frequency dependent studies were subsequently performed with the magnetic field applied within the easy plane in order to quantify the zfs parameters for complex **2**. Fig. 3 displays the positions of the observed EPR peaks plotted versus frequency. Superimposed on the data is the best fit to the above Hamiltonian; the curves correspond to the energy differences between levels connected by the arrows in the Zeeman diagram in Fig. 2. The obtained zfs parameters are:  $D = +0.62 \text{ cm}^{-1}$ ,  $g_{xy} = 2.00$  and a significant rhombic anisotropy,  $|E| \geq 0.067 \text{ cm}^{-1}$ . The obtained value of  $E$  is a lower limit, as the orientation of the field within the easy plane is not exactly known. In order to determine the precise value of  $E$ , angle-dependent studies would have to be performed within the easy plane. However, since this complex does not appear to be a SMM, such studies were not performed.

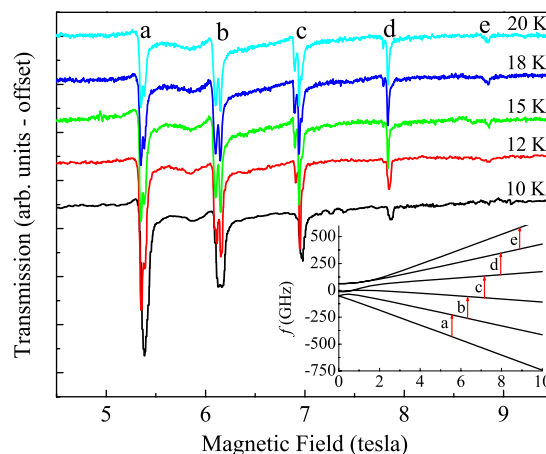


Fig. 2. Temperature-dependent EPR spectra of complex **2** taken at 197 GHz with the DC magnetic field applied within the easy plane. The inset shows the simulated Zeeman diagram for a positive  $D$  system. Transitions labeled 'a' (ground state transition) to 'e' in the spectra are also indicated in the inset. For the negative  $D$  case (see Fig. 3), the ground state transition would appear at the highest fields.

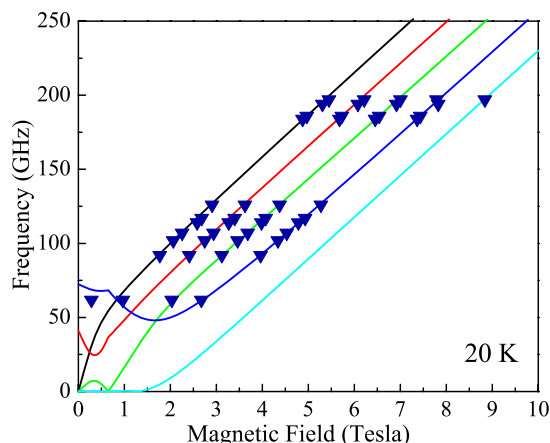


Fig. 3. Easy plane EPR peak positions for complex **2** plotted versus frequency. The solid lines are simulations using the *zfs* parameters given in the text.

On the other hand, complex **1** exhibits SMM-like EPR spectra. Fig. 4 shows single crystal data obtained at 51.8 GHz and at different temperatures, with the DC magnetic field applied within the hard-plane. Once again, five EPR peaks are observed (labeled 1–5), confirming the  $S = 5/2$  ground state of this molecule. The fact that the strongest peak is seen at the highest field (opposite to what was observed for complex **2**) indicates that  $D$  is negative. Another set of three weaker peaks can be seen as shoulders on three of the main peaks (labeled with subscripts  $x$ ). There are several possible explanations for these weaker peaks, including: a low lying  $S = 3/2$  excited state; intermolecular exchange interactions; or disorder-induced strains in the sample leading to different molecular species [10]. Recent calculations seem to exclude the possibility of low lying excited states [6]. However, further studies are required for precise determination of the origin of the weaker EPR peaks.

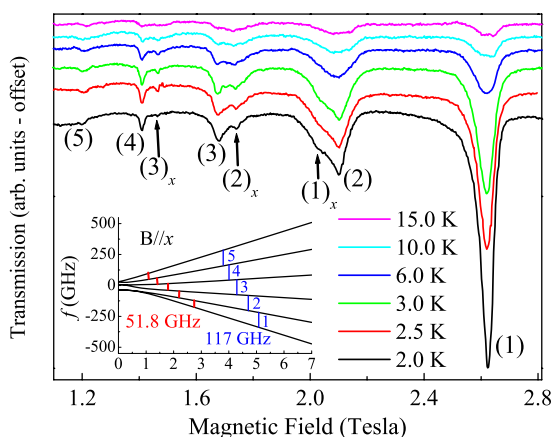


Fig. 4. HFEPR spectra of complex **1** taken at 51.8 GHz, at temperatures from 2 to 15 K. The inset shows the simulated Zeeman diagram for a negative  $D$  system. Transitions labeled (1) (ground state transition) to (5) in the spectra are also indicated in the inset for two different frequencies.

The inset to Fig. 4 shows the Zeeman diagram for a spin  $S = 5/2$  system with a negative  $D$  value and the field applied within the hard plane. The five observed transitions (1–5) are shown for two different EPR frequencies (51.8 and 117 GHz). Because the energy differences between Zeeman-split levels are much smaller at lower fields, less thermal energy is required to populate the higher-lying levels within the  $S = 5/2$  state. Higher frequency EPR

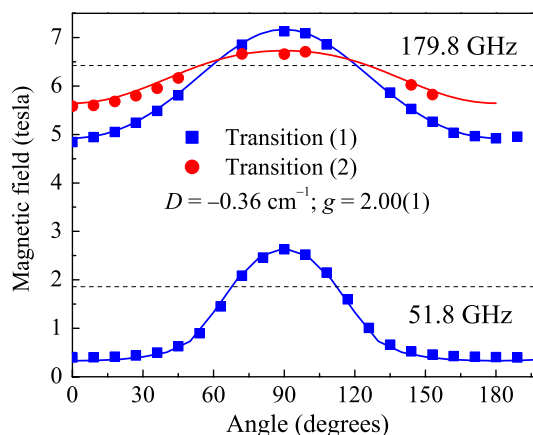


Fig. 5. Plot of the HFEPR peak positions for complex **1** obtained from angle-dependent measurements at 51.8 and 179.8 GHz, while rotating the field from the  $c$ -axis ( $0^\circ$ ) to the  $ab$ -plane ( $90^\circ$ ). The dashed lines represent the  $g = 2.00$  references for each frequency, and the solid lines are simulations with the given parameters.

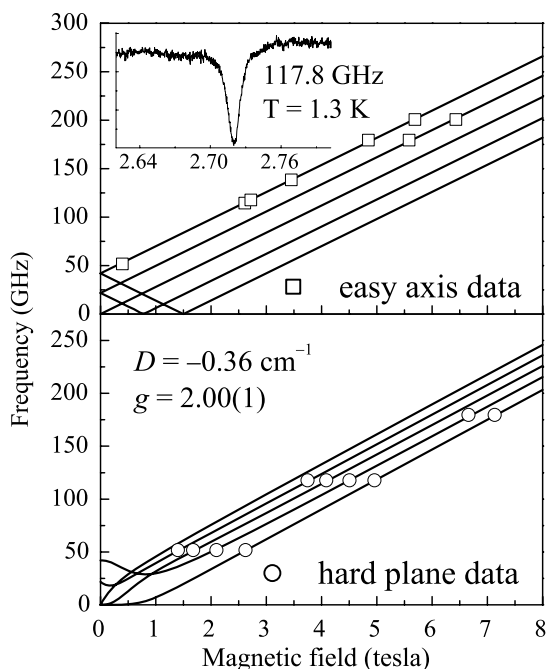


Fig. 6. Energy difference diagrams for complex **1** constructed from frequency-dependent measurements with the field along both the easy-axis and within the hard-plane. The solid lines are simulations with the given parameters. The inset shows a typical easy-axis EPR peak for a crystal of complex **1**, with a line width of about a hundred gauss.

spectra (not shown here) taken at 117.8 GHz show only peak (1) at 1.3 K.

Angle-dependent measurements from the *c*-axis to *ab*-plane were performed at 6 K, and frequencies of 51.8 and 179.8 GHz, as shown in Fig. 5. Superimposed on the data points are simulations using the following simple Hamiltonian (the parameters are listed in the figure):  $\hat{H} = D\hat{S}_z^2 + g\mu_B\vec{B} \cdot \hat{S}$ . The solid blue squares represent the transition from the ground state [labeled (1) in Fig. 4]; the red circles correspond to transition (2). The two dashed lines indicate the isotropic positions ( $D = 0$ ,  $g = 2.00$ ). The fact that the peaks shift approximately twice as far to the low field side of the  $g = 2.00$  reference, as compared to the high field side, implies a uniaxial anisotropy with a negative  $D$  parameter. Indeed, the high frequency data fit very well to a  $(1 - 3\cos^2\theta)$  angle dependence, which is expected for a SMM in the high field limit. The angle corresponding to  $\theta = 0^\circ$  marks the easy axis orientation.

Precise determination of the spin Hamiltonian parameters  $D$  and  $g$  is achieved through EPR spectra taken at various frequencies (50–200 GHz) for both the easy-axis and hard-plane orientations, as shown in Fig. 6. Simulations for both the easy-axis and hard-plane diagrams suggest that the system is best described with  $D = -0.36 \text{ cm}^{-1}$  and  $g = 2.00(1)$ . These parameters were used to simulate the angle-dependent EPR peak positions at 179.8 and 51.8 GHz, as shown in Fig. 5.

It is worth noting that the line width of the easy-axis EPR peak (inset of Fig. 6) is much sharper than the hard-plane ones. Further study is required to identify the cause of this difference. The easy-axis line width for complex **1** is  $\sim 0.01 \text{ T}$ , which is considerably narrower than other well studied SMMs [10,11]. The extraordinary sharpness of the EPR spectra seems to confirm the reduced decoherence in this system ( $T_2 \approx 3 \text{ ns}$ ) relative to other known SMMs, thus making it an interesting candidate for studies of coherent quantum magnetization dynamics.

#### 4. Summary and conclusions

On the basis of detailed frequency and field orientation dependent HFEPR studies, we show that  $[\text{Fe}_7\text{O}_3(\text{O}_2\text{C-Bu}^t)_9(\text{mda})_3(\text{H}_2\text{O})_3]$  (**1**) represents a rare example of a half-integer-spin ( $S = 5/2$ ) iron SMM, having a negative uniaxial zero-field-splitting parameter  $D = -0.36 \text{ cm}^{-1}$ . Meanwhile,  $[\text{Fe}_7\text{O}_4(\text{O}_2\text{CPh})_{11}(\text{dmem})_2]$  (**2**) is not a SMM. The EPR linewidth for complex **1** is considerably narrower in comparison to spectra obtained for other SMMs, making it an interesting candidate for studies of coherent quantum magnetization dynamics.

#### Acknowledgement

This work was supported by the US National Science Foundation under Grant numbers DMR-0239481, DMR-0414809 and DMR-0506946.

#### References

- [1] J.R. Friedman, M.P. Sarachik, J. Tejada, R. Ziolo, Phys. Rev. Lett. 76 (1996) 3830.
- [2] L. Thomas, F. Lionti, R. Ballou, D. Gatteschi, R. Sessoli, B. Barbara, Nature 383 (1996) 145.
- [3] R. Sessoli, A. Caneschi, D. Gatteschi, L. Sorace, A. Cornia, W. Wernsdorfer, J. Magn. Mater. 226 (2001) 1954.
- [4] S. Hill, R.S. Edwards, N. Aliaga-Alcalde, G. Christou, Science 302 (2003) 1015.
- [5] N. Aliaga-Alcalde, R. Edwards, S. Hill, W. Wernsdorfer, K. Foelting, G. Christou, J. Am. Chem. Soc. 126 (2004) 12503.
- [6] D. Foguet-Albiol, T.A. O'Brien, W. Wernsdorfer, S.C. Lee, S. Hill, K.A. Abboud, G. Christou, in preparation.
- [7] R. Bagai, S. Datta, A. Betancur Rodriguez, S. Hill, K.A. Abboud, G. Christou, in preparation.
- [8] M. Mola, S. Hill, P. Goy, M. Gross, Rev. Sci. Instrum. 71 (2000) 186.
- [9] S. Takahashi, S. Hill, Rev. Sci. Instrum. 76 (2005) 023114.
- [10] S. Hill, S. Maccagnano, K. Park, R.M. Achey, J.M. North, N.S. Dalal, Phys. Rev. B 65 (2002) 224410.
- [11] J. Lawrence, S. Hill, C. Kirman, E.-C. Yang, D. Hendrickson, R. Edwards, A. Yamaguchi, H. Ishimoto, W. Wernsdorfer, C. Ramsey, N.S. Dalal, M. Olmstead, in preparation.